batteries

MDPI

Article

Preparation and Properties of PP/PAN/Cotton Fibers Composite Membrane as Lithium-Ion Battery Separator with Thermal Shut-Off Function

Peiyu Liu, Xiongfei Zhang *, Chuang Ma, Dan Huang, Pengyun Li, Yana Shi, Chunxiao Qu and Xiang Shi

College of Chemistry and Chemical Engineering, Changsha University of Science and Technology, Changsha 410114, China

* Correspondence: zxf0902@csust.edu.cn; Tel.: +86-13974919886

Abstract: The lithium-ion battery separator plays roles of separating the positive and negative electrodes and providing ion channels, and at the same time, it can play a more important role in the safety of the lithium-ion battery. In this work, a modified PP (polypropylene)/PAN (polyacrylonitrile)/cotton fibers composite membrane with a thermal shut-off function was prepared by a wet-laid process. The results are as follows: When the fibers' mass fraction was 50%, the composite membrane had the best combination properties, with a tensile strength of 1.644 KN·m^{-1}, the porosity was 63%, and it had good wettability with an aspiration height of 39 mm and a liquid absorption rate of 269%. The thermal shrinkage of the composite membrane was less than 4% after thermal treatment under 160 °C. More importantly, the DSC curve showed that the modified PP/PAN/cotton fibers composite membrane had a thermal shut-off function with the temperature between 110 °C and 160 °C. After thermal treatment under 160 °C for 1 h, the ionic conductivity of the fiber membrane decreased to 0.32 mS·cm^{-1} from 1.99 mS·cm^{-1}. Electrochemical performance tests showed that the button battery using the fiber composite membrane had a slightly better initial discharge, capacity retention and cycle performance at different rates than the button battery equipped with the PP membrane. The results show that the modified PP/PAN/cotton fibers composite membrane improves the safety and electrochemical performance of lithium-ion battery.

Keywords: PP fiber; PAN fiber; lithium-ion battery separator; thermal shut-off

Citation: Liu, P.; Zhang, X.; Ma, C.; Huang, D.; Li, P.; Shi, Y.; Qu, C.; Shi, X. Preparation and Properties of PP/PAN/Cotton Fibers Composite Membrane as Lithium-Ion Battery Separator with Thermal Shut-Off Function. *Batteries* **2023**, *9*, 113. https://doi.org/10.3390/batteries9020113

Academic Editor: Carlos Ziebert

Received: 25 December 2022
Revised: 27 January 2023
Accepted: 2 February 2023
Published: 5 February 2023

1. Introduction

The lithium-ion battery has been recognized as one of the best energy storage devices of the future and has been widely used in digital products, including cell phones [1], laptops [2], wearable devices [3,4] and model airplanes [5] because of their high energy density compared to other commercial rechargeable batteries [6]. However, their safety performance and ionic conductivity remain two challenges for them to be used for large-scale energy storage for electric automobiles and smart grids [7,8].

The separator, a pivotal part of a lithium-ion battery, plays a vital role in the separation of the anode and cathode to prevent a short circuit inside the battery [9,10], but also, it should have high wettability and good permeability to the electrolyte for efficient ion transport [11–13].

Among the different types of separators, such as microporous polymer membrane [14,15], modified microporous polymer composite membrane [16–21], nonwoven membrane [22–26] and aerogel membrane [27–29], commercial polyolefin microporous membranes, such as polypropylene (PP), polyethylene (PE) and PP/PE/PP, have been extensively applied to lithium-ion batteries because of their superior mechanical strength and electrochemical stability [30–34]. However, their lower ionic conductivity, lower porosity and higher thermal shrinkage limit their application [35–38].

A nonwoven membrane with web structures is bonded together by entangled small diameter fibers produced by melt-blown, wet-laid and electrospinning technologies [39–44]; therefore, it shows a higher porosity [45–47].

There are a significant number of -OH polar groups contained on cotton fibers, which makes their hydrophilicity excellent; polyacrylonitrile (PAN) fibers have -CN hydrophilic groups, and their melting point is high, up to 320 °C. It is proposed that modified PP fibers [48], cotton fibers and PAN fibers are used as raw materials, the separator is prepared with a wet-laid process, the thickness of the separator is controlled by regulating the amount of fibers, and the porosity and wettability of the separator are also adjusted by changing the fibers' ratio. At the same time, the higher melting point of the PAN fibers can be used as a skeleton material to improve the separator's shape retention ability and decrease its degree of thermal shrinkage. More importantly, the lower melting point components are susceptible to melting and diffusion, which can block the pores of the separator, thereby decreasing the porosity, decreasing the electrical conductivity and having a "thermal shut-off" effect, thus considerably improving battery safety.

Through the above research, we expect to obtain a new production process for a lithium-ion battery separator with a low cost and high level of safety to meet the sustainable development requirements.

2. Materials and Methods

2.1. Experimental Materials

PAN fibers: 2~5 mm, Changsha Bosset Construction Engineering Materials Co., Ltd. (Changsha, China); Degreasing Cotton: Premium grade, Hengshui Chaoshun Sanitary Materials Co., Ltd. (Hengshui, China); PP fibers: 5 mm, Taian Tonghong Fibers Co., Ltd. (Taian, China); polyethylene oxide (PEO): molecular weight 5 million, Jilin Global Fine Chemical Co., Ltd. (Jilin, China); polyvinyl alcohol (PVA): analytically pure, Sinopharm Chemical Reagent Co., Ltd. (Shanghai, China); ethylene carbonate (EC): analytical grade, Tianjin Institute of Chemical Reagents (Tianjin, China); dimethyl carbonate (DMC): analytical grade, Tianjin Institute of Chemical Reagents; hexadecane: analytical grade, Tianjin City Chemical Reagent Institute.

2.2. Preparation of Modified PP/PAN/Cotton Fibers Composite Membrane

PP fibers were modified by graft coating to improve the dispersibility and density of the PP fibers in water. Using a wet-laid process, PP and PAN fibers were mixed with degreased cotton fibers after pulping in a certain ratio, and the required amount of mixed fibers was calculated using a separator having a unit weight of 30 $g \cdot m^{-2}$. Using a fibers disintegrator to disperse, a certain amount of dispersant polyoxyethylene (PEO) and binder polyvinyl alcohol (PVA) were added to the mixed slurry, and the slurry was evenly stirred, and then formed into a sheet on a sheet former. Then it was hot pressed to form a separator. The flow chart is shown in Figure 1.

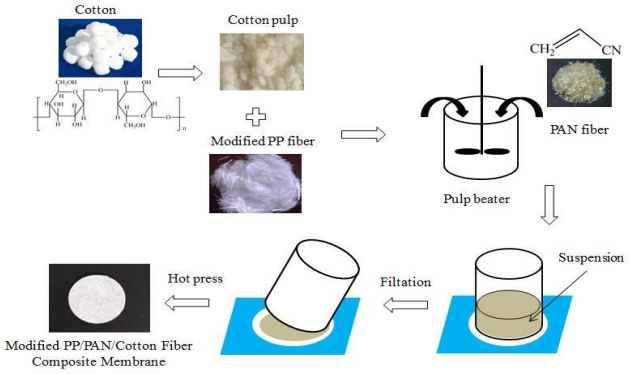

Figure 1. The process for modified PP/PAN/cotton fibers composite membrane.

2.3. Characterization Methods

Tensile strength was measured under the rate of 20 mm·min^{-1} by WZL-300B tensile strength instrument, and the test specimens were 15 mm × 100 mm in size. Since the separator can be considered as a two-dimensional material, the tensile strength measured in KN·m^{-1} as a unit can be obtained by dividing the breaking length by the tensile force.

Surface morphologies of separator were studied by scanning electron microscopy (SEM, FEI Quanta-200).

Porosity of the membrane was measured by absorption method of n-hexadecane [22,44]. Firstly, the septum samples were dried in oven at 100–105 °C for 2 h, taken out, cooled. After that, they were soaked in n-hexadecane for 1 h, removed and remaining liquid on their surface was wiped off by filter paper. Separator porosity (P) was calculated using Equation (1):

$$P = \frac{m_t - m_0}{\rho V} \times 100\% \quad (1)$$

where m_t and m_0 are the separator mass after and before immersing in n-hexadecane for 1 h, respectively, ρ is the n-hexadecane density, V is the separator volume.

The electrolyte uptake was determined by weighing the separator before and after the electrolyte. Separator electrolyte uptake (E) was determined by Equation (2):

$$E = \frac{m_1 - m_0}{m_0} \times 100\% \quad (2)$$

where m_1 and m_0 are the separator weights after and before immersion in electrolyte, respectively.

Make a line at 5 mm from the end of the separator (15 mm × 100 mm), then hang the upper end of the separator vertically on the iron stand, and slowly immerse the end of the separator in the electrolyte solution until the mark is flush with the liquid level. After 10 min, the liquid climb height is measured, and the average value is taken as the electrolyte absorption height.

The melt peak and crystallization peak of the composite membrane were tested under N_2 atmosphere with the temperature rise rate of 10 °C/min, by differential scanning calorimetry (DSC) using a comprehensive thermal analyzer model STA449-F3 from NETZSCH, Waldkraiburg, Germany.

In order to analyze the heat shrinkage behavior of separator, it was put in the oven and heated at 160 °C for 1 h. Separator thermal shrinkage (T) was determined by Equation (3):

$$T = \frac{S_1 - S_0}{S_1} \times 100\% \quad (3)$$

where S_1 and S_0 are the separator area after and before thermal treatment, respectively.

The AC impedance was measured on an electrochemical workstation with the separator sandwiched between two stainless electrodes and soaked in electrolyte with a frequency range of 1 Hz–100 kHz and AC amplitude of 5 mV at room temperature, while a saturated glycerol electrode was applied as reference electrode. Thus, the ionic conductivity of the separator was determined by immersion in an electrolyte (1 M LiPF6/ EC: DMC = 1:1 (v/v)). In the AC impedance spectra, the impedance of the sample under test is the intersection of the high frequency curve with the coordinate axis, and the impedance of the membrane is the difference between the impedance common to the membrane and electrolyte system and the impedance of the electrolyte [49,50]. Ionic conductivity (σ) was determined by the following Equation (4):

$$\sigma = \frac{d}{R_b \times A} \quad (4)$$

where d and A are thickness and effective area of the membrane, respectively, and R_b is the resistance of bulk electrolyte.

Ternary cathode materials $LiNi_{0.8}Co_{0.1}Mn_{0.1}O_2$ 0.3200 g, polyvinylidene fluoride 0.0400 g and acetylene black 0.0400 g were added in the mass ratio of 8:1:1, mixed and

ground into black paste, coated on aluminum foil, dried and cut into 14 mm cathode sheets. Button batteries consist of cathode sheet, lithium metal sheet, nickel mesh, electrolyte and composite membrane prepared in this study or PP separator. The effect of membrane on discharge capacity, cycling performance and rate capability of the battery was studied using a LAND test system.

3. Results and Discussion

3.1. Mechanical Properties of the Separator

Figure 2 is shows the effect of the modified PP and PAN fibers and cotton fibers on the tensile strength of the composite membrane according to different mass ratios. It can be shown that as the mass fraction of the modified PP and PAN fibers increases, the tensile strength of the fiber membrane also increases. This makes them more stable to improve the quality of the membranes produced by the wet-laid process, and good experimental reproducibility is indicated by the standard deviation of less than 0.048 obtained from three repetitions of each group as shown in Table 1. Since the tensile strengths of the PP and PAN fibers are larger than the tensile strength of the cotton fibers, they are mixed with the cotton fibers; the fibers are interwoven and the cotton fiber chain contains a significant amount of -OH polar groups. Hydrogen bonds are formed between the cotton fibers, thereby increasing the tensile strength of the composite membrane. When the mass fraction of the PP and PAN fibers in the membrane is 30%, the membrane's tensile strength is greater than 1.5 KN·m^{-1}. Continuing to increase the fiber content of PP and PAN does not contribute much to improving the tensile strength of the composite separator. At the same time, the hydrogen bonds formed are gradually reduced, and the interweaving force between the fibers is also lowered. Therefore, the tensile strength of the fiber separator is not enlarged much. However, the composite membrane's tensile strength with fiber ratios of 30–70% can achieve normal use in a lithium-ion battery.

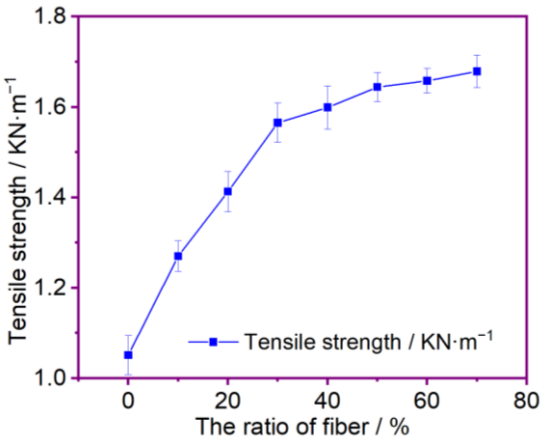

Figure 2. The effect of fibers' ratio for tensile strength.

Table 1. Physical properties of composite membranes with different fiber ratios.

The Ratio of Fibers/%	Mean Value of Tensile Strength/KN·m^{-1}	Standard Deviation of Tensile Strength/KN·m^{-1}	Porosity/%	Electrolyte Uptake/%	Absorbent Height/mm	Thermal Shrinkage/%
0	1.051	0.0430	25	183	15	3.9
10	1.270	0.0333	32	192	20	3.45
20	1.413	0.0445	41	205	23	2.88
30	1.565	0.0434	46	234	26	2.53
40	1.599	0.0480	52	249	32	2.1
50	1.644	0.0321	63	269	39	1.95
60	1.658	0.0272	68	221	35	1.9
70	1.679	0.0362	72	180	38	1.87

3.2. The Porosity of the Separator

Figure 3 shows the effect of the fiber ratio on the porosity of the fiber membrane. It can be shown that the porosity of the membrane increases as the mass fraction of the modified PP and PAN fibers increases. The cotton fibers are fibrillated and dispersed into fine fibers, while the diameters of the modified PP and PAN fibers are relatively large. Because the separator obtained is formed by the uniform and random accumulation of fibers, the larger pores are formed by larger diameter fibers between them, and the corresponding porosity is relatively larger. Therefore, as the mass fraction of the modified PP and PAN fibers increases, the porosity also increases. When the mass fraction of the PP and PAN fibers goes from 40% to 50%, it is significant to see the rise in porosity. However, the growth rate of porosity decreases when the mass fraction of the PP and PAN fibers goes from 50% to 70%; their porosity is more than 60%, which can be used for a normal Li-ion battery. The data on the membrane's porosities that correspond to the different fiber ratios are presented in Table 1.

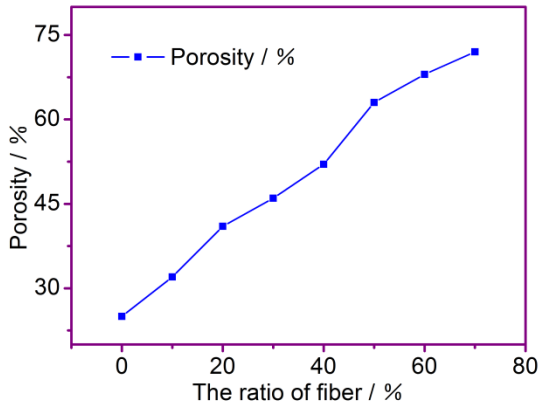

Figure 3. The effect of ratio of fibers on porosity.

3.3. The Liquid Absorption of the Separator

The contribution of the ability of the separator to be wetted by the electrolyte to the separator conductivity is significant. The membrane absorption ability to the electrolyte is reflected by the liquid absorption rate of the membrane, and the membrane absorption speed to the electrolyte is reflected by the liquid absorption height. It can be shown from Figure 4 that the liquid absorption rate of the fiber membrane increases as the mass fraction of the modified PP fibers and PAN fibers increases. When the mass fraction is 50%, the liquid absorption rate reaches a maximum of 269%. Then, the liquid absorption rate of the composite membrane is gradually lowered. This is mainly because the PAN fibers contain a significant amount of polar groups (-CN), and the surface of the modified PP fibers is also grafted with a polar group, which has good hydrophilic properties and better hygroscopicity. The cotton fibers can be used together to greatly improve the hydrophilic performance and the liquid absorption speed of the separator. When the mass fraction of the modified PP fibers and the PAN fibers is 50%, the aspiration height is 39 mm. However, when the liquid absorption rate of the fiber membrane reaches a certain height, the liquid absorption rate of the fiber membrane is gradually decreased as the cotton fibers gradually decrease. It will also be reduced. When the mass fraction of the modified PP fibers and PAN fibers is 50%, the liquid absorption performance is the best: the liquid absorption rate is 269%, and the liquid absorption height is 39 mm. The other data on the electrolyte uptake and absorbent height of the separators, which correspond to different fiber ratios, are presented in Table 1.

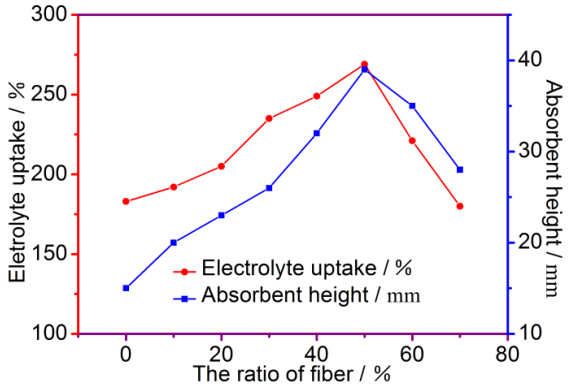

Figure 4. The effect of fiber ratio on electrolyte uptake.

3.4. Thermal Shrinkage of the Separator

Figure 5 shows the thermal shrinkage of the composite separators with different fiber ratios after treatment at 160 °C for 1 h. It can be shown from the figure that the PP/PAN/cotton fibers composite membrane has a shrinkage of less than 4% at 160 °C, and as the content of the modified PP fibers and PAN fibers increases, i.e., when the content of the modified PP fibers and PAN fibers is higher than 50%, the change in shrinkage tends to be stable to less than 2%. This is mainly because the PAN fibers form a skeleton of the separator, and the separator is not easily shrunk after thermal treatment. Relevant data on the thermal shrinkage of fiber membranes that correspond to different fiber ratios are presented in Table 1.

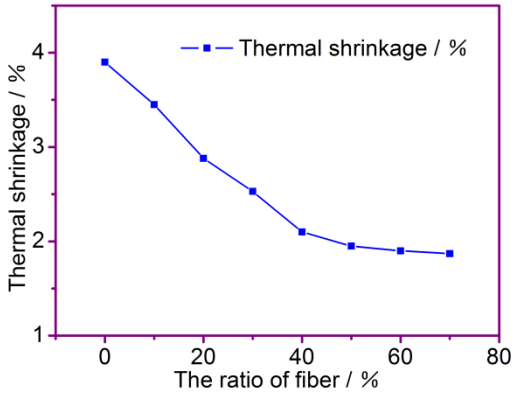

Figure 5. The effect of fiber ratio on thermal shrinkage at 160 °C.

We need the membrane to have the best hydrophilicity and thermal stability while satisfying the premise of having good tensile strength and porosity. Therefore, the composite membrane with a 50% ratio of modified PP fibers and PAN fibers was determined to have the best overall performance based on a comprehensive analysis of data such as tensile strength, porosity, hydrophilicity and thermal stability, and was continued to be analyzed in the following tests.

3.5. Thermal Shut-Off Performance of the Separator

To achieve the thermal shut-off performance of the membrane, PP fibers and PAN fibers with different melting points were mixed with cotton fibers. Cotton fibers were used as the substrate of the separator, PP fibers were used as the low melting point component and PAN fibers were used as the high melting point component and the skeleton material of the separator. The thermal shut-off temperature range and thermal shut-off process of the separator are discussed in terms of DSC, conductivity and SEM image.

Figure 6 is a DSC curve of the modified PP/PAN/cotton fibers composite membrane. It can be shown that the endothermic peak about 110 °C is the melting peak of PP, and

the exothermic peak at around 160 °C is the crystallization peak of PAN. The endothermic peak around 280 °C is the melting peak of PAN. In summary, the melting point of PAN is considerably higher than that of PP. Thus, as the temperature gradually rises to 110 °C and continues to rise to below 160 °C, PP fibers melt and flow first, blocking the pores of the separator, and the interdigitation of the PAN fibers and cotton fibers can maintain the structural integrity of the separator, thereby achieving the battery thermal shut-off function. Therefore, the thermal closure temperature of the separator ranges from 110 °C to 160 °C.

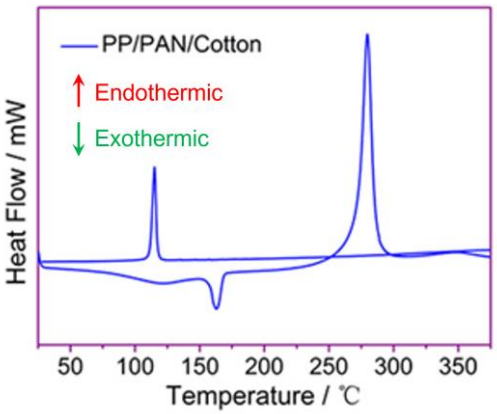

Figure 6. DSC curves of modified PP/PAN/cotton fibers composite membrane.

Figure 7 shows the AC impedance spectrum of the modified PP/PAN/cotton fibers composite membrane before and after treatment at 160 °C. In previous reports, the impedance and conductivity of the PP membrane were 1.50 Ω and 0.68 mS·cm^{-1} at room temperature, respectively [43]. From the figure, before thermal treatment, it can be seen that the impedance of the fiber membrane was lower compared to the impedance of the PP membrane, which was 1.03 Ω, and the fiber membrane conductivity obtained by calculation was σ = 1.99 mS·cm^{-1}, which was much higher than the conductivity of the PP membrane. These results are due to the remarkable liquid absorption and high porosity of the fiber membrane. After treatment at 160 °C, the impedance of the separator was 6.24 Ω and the conductivity was 0.32 mS·cm^{-1}. This is because the PP fibers in the separator melt and block the pores of the membrane after thermal treatment, increasing the membrane resistance and preventing the transport of lithium-ions. When the battery interior temperature continues to rise, the thermal closure function of the membrane acts, the ionic conductivity decreases, the reaction slows down and the temperature stops rising or falling, which can avoid a series of subsequent safety problems.

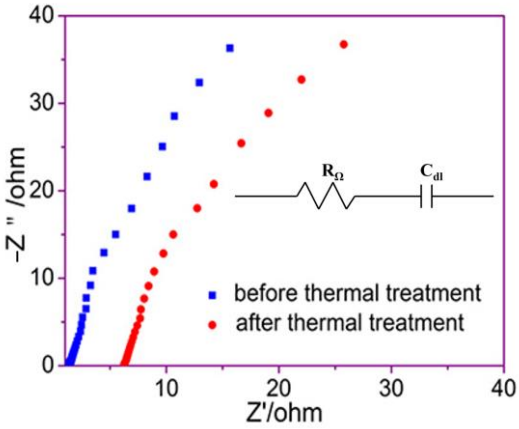

Figure 7. AC impedance spectra of fiber membrane before and after thermal treatment.

Figure 8 shows a scanning electron micrograph of before (a) and after (b, c) thermal treatment at 160 °C for 0.5 h of a modified PP/PAN/cotton fibers composite membrane.

In Figure 8a, the modified PP fibers, PAN fibers and cotton fibers are interlaced to form uniform and orderly pores. The modified PP fibers are modified by graft coating, and the surface has many fine particles. PAN fibers have a smooth appearance, and due to the polar cyano group (-CN), the PAN fibers have excellent wettability; the intertwining of the fibers increases the membrane tensile strength. As shown in Figure 8b,c, after thermal treatment at 160 °C, the PP fibers melt and diffuse, blocking the composite separator pores, and the membrane porosity is reduced, but the PAN fibers and the cotton fibers can still interweave to form the separator. The skeleton ensures that the shape of the separator does not change after the PP is melted at a high temperature, and the adhesion between the PAN fibers and the cotton fibers can be increased after the PP is melted. In the battery, when the temperature rises, the separator pores become smaller and smaller, which can prevent the electrochemical reaction from proceeding and prevent thermal runaway.

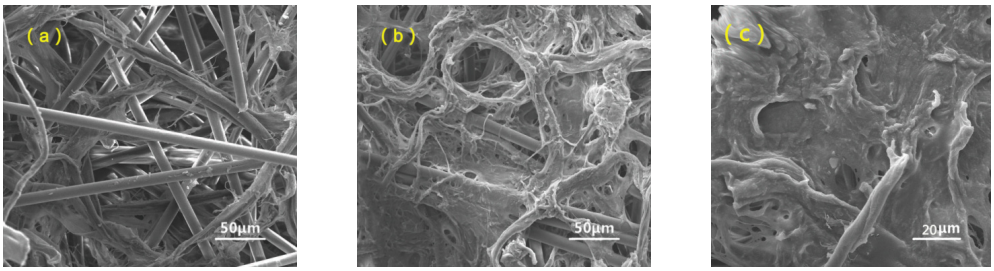

Figure 8. SEM of modified PP/PAN/cotton fibers composite membrane: (**a**) before thermal treatment; (**b**,**c**) after thermal treatment.

3.6. Electrochemical Performance of the Separator

Figure 9 shows the initial charge–discharge curve of the lithium-ion batteries using the PP membrane and the modified PP/PAN/cotton fibers composite membrane at 1 C rate, respectively. It is shown that the initial discharge capacities of the batteries with the PP membrane and the modified PP/PAN/cotton fibers composite membrane were 165.8 mAh·g^{-1} and 166.7 mAh·g^{-1}, respectively. Compared with the cell using the commercial PP membrane, the cell using the modified PP/PAN/cotton fibers composite membrane had a slightly higher initial charge–discharge capacity, which is due to the improvement in the electrolyte wettability of the composite membrane. Furthermore, the ionic conductivity of the composite membrane is improved, which is advantageous for the improvement in the charge and discharge performance of the battery.

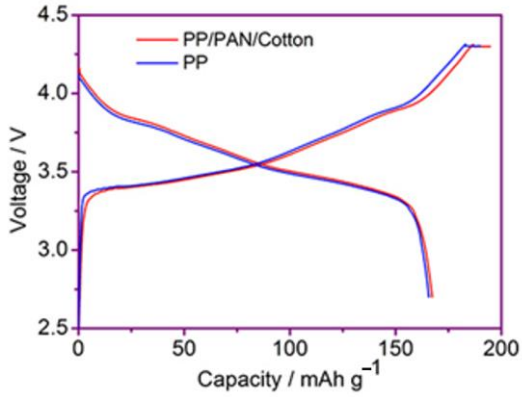

Figure 9. Initial charge–discharge curves of the cell using PP membrane and modified PP/PAN/cotton fibers composite membrane.

Figure 10 is the graph of the 100 cycle performance of Li-ion batteries using the PP membrane and the modified PP/PAN/cotton fibers composite membrane under 1 C rate. The discharge capacity of the cell by the PP membrane after 100 cycles is 153.4 mAh·g^{-1}, and the capacity retention rate is 92.5%. The discharge capacity of the battery by the fiber

membrane after 100 cycles is 156.5 mAh·g^{-1}, and the capacity retention rate is 93.8%, which is slightly higher than that of the battery using the PP membrane. This may be due to an increase in the ionic conductivity of the composite membrane. Under the premise of realizing the thermal closure function of the membrane, it does not affect the performance of transporting lithium-ions of the separator at a normal operating temperature.

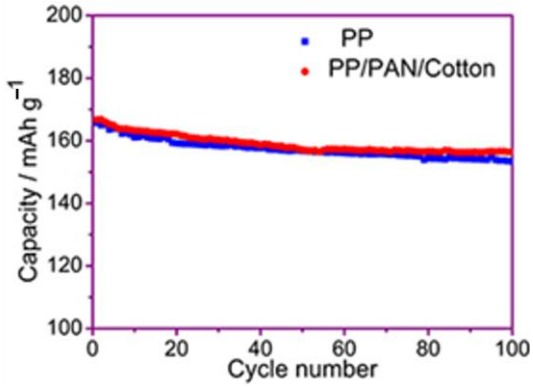

Figure 10. Cycle performance of the batteries by PP membrane and modified PP/PAN/cotton fibers composite membrane.

Rate capability is shown by Figure 11 for batteries using PP membranes and the fiber membrane at different rates of 1 C, 2 C and 5 C. Compared to PP membranes, the battery with fiber membranes has a slightly higher rate capability at different C rates. The specific energies of the cells with fiber and PP membranes are 166.7 mAh·g^{-1} and 165.8 mAh·g^{-1} at 1 C, 153.2 mAh·g^{-1} and 151.0 mAh·g^{-1} at 2 C, and 130.3 mAh·g^{-1} and 128.1 mAh·g^{-1} at 5 C, respectively. When the rate is back to 1 C again, the batteries with fiber and PP membranes have capacities of 159.3 mAh·g^{-1} and 156.8 mAh·g^{-1}, respectively, which are nearly the same as their original capacities. It is interpreted that this result is significant for the effect on ion transport. The rate capability of the battery using the fiber membrane is a bit better than the battery with the PP membrane. The enhanced rate capability is attributed to the higher ion conductivity of the fiber membrane.

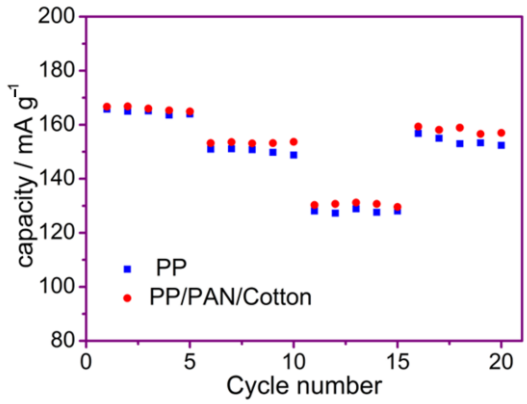

Figure 11. Rate capability of the batteries with PP membrane and fiber membrane.

4. Conclusions

In this paper, the modified PP/PAN/cotton fibers composite membrane with a thermal shut-off function is prepared by a wet-laid process. Through the separator's basic performance test, it was concluded that the best overall performance of the separator was achieved when the mass fraction of the modified PP fibers and PAN fibers was 50%. The separator has the best electrolyte wettability with an absorption height of 39 mm and an electrolyte uptake of 269%; meanwhile, the porosity of the membrane reached 63%, which makes the membrane exhibit a high ionic conductivity of 1.99 mS·cm^{-1}, and excellent

mechanical performance was also achieved with a tensile strength of 1.644 KN·m^{-1}. The membrane has excellent thermal dimensional stability, and the thermal shrinkage of the membrane under the optimal proportioning conditions is only less than 2% when treated at 160 °C for 0.5 h. Most important of all, the separator possesses a thermal shut-off function under the temperature between 110~160 °C, and the ionic conductivity of the separator decreases to 0.32 mS·cm^{-1}, which significantly decreases the battery's reaction rate and prevents a further increase in the battery's temperature, thus improving the battery's safety. Meanwhile, the lithium-ion battery equipped with the fiber membrane had a better initial charge, discharge capacities, capacity retention and cycle performance at different rates compared with the battery equipped with the PP membrane.

Author Contributions: Conceptualization, P.L. (Peiyu Liu) and X.Z.; methodology, X.Z.; software, P.L. (Peiyu Liu); validation, C.M., D.H. and Y.S.; formal analysis, C.Q.; investigation, X.S.; resources, X.Z.; data curation, P.L. (Pengyun Li); writing—original draft preparation, P.L. (Peiyu Liu); writing—review and editing, X.Z.; visualization, C.M.; supervision, D.H.; project administration, P.L. (Peiyu Liu); funding acquisition, X.Z. All authors have read and agreed to the published version of the manuscript.

Funding: This research received no external funding.

Institutional Review Board Statement: Not applicable.

Informed Consent Statement: Not applicable.

Data Availability Statement: Not applicable.

Conflicts of Interest: The authors declare no conflict of interest.

References

1. Duh, Y.-S.; Lin, K.H.; Kao, C.-S. Experimental investigation and visualization on thermal runaway of hard prismatic lithium-ion batteries used in smart phones. *J. Therm. Anal. Calorim.* **2018**, *132*, 1677–1692. [CrossRef]
2. Sabbaghi, M.; Esmaeilian, B.; Raihanian Mashhadi, A.; Cade, W.; Behdad, S. Reusability Assessment of Lithium-Ion Laptop Batteries Based on Consumers Actual Usage Behavior. *J. Mech. Des.* **2015**, *137*, 124501. [CrossRef]
3. Dong, X.; Chen, L.; Su, X.; Wang, Y.; Xia, Y. Flexible Aqueous Lithium-Ion Battery with High Safety and Large Volumetric Energy Density. *Angew. Chem. Int. Ed.* **2016**, *55*, 7474–7477. [CrossRef]
4. Ren, J.; Li, L.; Chen, C.; Chen, X.; Cai, Z.; Qiu, L.; Wang, Y.; Zhu, X.; Peng, H. Twisting Carbon Nanotube Fibers for Both Wire-Shaped Micro-Supercapacitor and Micro-Battery. *Adv. Mater.* **2013**, *25*, 1155–1159. [CrossRef] [PubMed]
5. Hollinger, A.S.; McAnallen, D.R.; Brockett, M.T.; DeLaney, S.C.; Ma, J.; Rahn, C.D. Cylindrical lithium-ion structural batteries for drones. *Int. J. Energy Res.* **2020**, *44*, 560–566. [CrossRef]
6. Wang, R.; Li, X.; Wang, Z.; Zhang, H. Electrochemical analysis graphite/electrolyte interface in lithium-ion batteries: p-Toluenesulfonyl isocyanate as electrolyte additive. *Nano Energy* **2017**, *34*, 131–140. [CrossRef]
7. Liu, B.; Jia, Y.; Li, J.; Yin, S.; Yuan, C.; Hu, Z.; Wang, L.; Li, Y.; Xu, J. Safety issues caused by internal short circuits in lithium-ion batteries. *J. Mater. Chem. A* **2018**, *6*, 21475–21484. [CrossRef]
8. Li, Y.; Li, Q.; Tan, Z. A review of electrospun nanofiber-based separators for rechargeable lithium-ion batteries. *J. Power Sources* **2019**, *443*, 227262. [CrossRef]
9. Zhang, Y.; Qiu, Z.; Wang, Z.; Yuan, S. Functional polyethylene separator with impurity entrapment and faster Li^+ ions transfer for superior lithium-ion batteries. *J. Colloid Interface Sci.* **2022**, *607*, 742–751. [CrossRef]
10. Lagadec, M.F.; Zahn, R.; Wood, V. Characterization and performance evaluation of lithium-ion battery separators. *Nat. Energy* **2019**, *4*, 16–25. [CrossRef]
11. Parikh, D.; Jafta, C.J.; Thapaliya, B.P.; Sharma, J.; Meyer, H.M.; Silkowski, C.; Li, J. Al_2O_3/TiO_2 coated separators: Roll-to-roll processing and implications for improved battery safety and performance. *J. Power Sources* **2021**, *507*, 230259. [CrossRef]
12. Ding, L.; Xu, G.; Ge, Q.; Wu, T.; Yang, F.; Xiang, M. Effect of Fumed SiO_2 on Pore Formation Mechanism and Various Performances of β-iPP Microporous Membrane Used for Lithium-ion Battery Separator. *Chin. J. Polym. Sci.* **2018**, *36*, 536–545. [CrossRef]
13. Xiang, Y.; Li, J.; Lei, J.; Liu, D.; Xie, Z.; Qu, D.; Li, K.; Deng, T.; Tang, H. Advanced Separators for Lithium-Ion and Lithium–Sulfur Batteries: A Review of Recent Progress. *ChemSusChem* **2016**, *9*, 3023–3039. [CrossRef] [PubMed]
14. Li, Y.; Pu, H.; Wei, Y. Polypropylene/polyethylene multilayer separators with enhanced thermal stability for lithium-ion battery via multilayer coextrusion. *Electrochim. Acta* **2018**, *264*, 140–149. [CrossRef]
15. Ding, L.; Zhang, C.; Wu, T.; Yang, F.; Lan, F.; Cao, Y.; Xiang, M. Effect of temperature on compression behavior of polypropylene separator used for Lithium-ion battery. *J. Power Sources* **2020**, *466*, 228300. [CrossRef]

16. Fu, W.; Xu, R.; Zhang, X.; Tian, Z.; Huang, H.; Xie, J.; Lei, C. Enhanced wettability and electrochemical performance of separators for lithium-ion batteries by coating core-shell structured silica-poly(cyclotriphosphazene-co-4,4′-sulfonyldiphenol) particles. *J. Power Sources* **2019**, *436*, 226839. [CrossRef]
17. Zhang, Z.; Yuan, W.; Li, L. Enhanced wettability and thermal stability of nano-SiO_2/poly(vinyl alcohol)-coated polypropylene composite separators for lithium-ion batteries. *Particuology* **2018**, *37*, 91–98. [CrossRef]
18. Li, J.; Wang, Q.; Wang, Z.; Cao, Y.; Zhu, J.; Lou, Y.; Zhao, Y.; Shi, L.; Yuan, S. Evaporation and in-situ gelation induced porous hybrid film without template enhancing the performance of lithium ion battery separator. *J. Colloid Interface Sci.* **2021**, *595*, 142–150. [CrossRef]
19. Kim, P.S.; Le Mong, A.; Kim, D. Thermal, mechanical, and electrochemical stability enhancement of Al_2O_3 coated polypropylene/polyethylene/polypropylene separator via poly(vinylidene fluoride)-poly(ethoxylated pentaerythritol tetraacrylate) semi-interpenetrating network binder. *J. Membr. Sci.* **2020**, *612*, 118481. [CrossRef]
20. Su, M.; Chen, Y.; Wang, S.; Wang, H. Bifunctional separator with high thermal stability and lithium dendrite inhibition toward high safety lithium-ion batteries. *Chin. Chem. Lett.* **2022**. [CrossRef]
21. Qi, X.; Zhang, Z.; Tu, C.; Zhu, C.; Wei, J.; Yang, Z. Covalent grafting interface engineering to prepare highly efficient and stable polypropylene/mesoporous SiO_2 separator for Li-ion batteries. *Appl. Surf. Sci.* **2021**, *541*, 148405. [CrossRef]
22. Huang, X. Performance evaluation of a non-woven lithium ion battery separator prepared through a paper-making process. *J. Power Sources* **2014**, *256*, 96–101. [CrossRef]
23. Hao, J.; Lei, G.; Li, Z.; Wu, L.; Xiao, Q.; Wang, L. A novel polyethylene terephthalate nonwoven separator based on electrospinning technique for lithium ion battery. *J. Membr. Sci.* **2013**, *428*, 11–16. [CrossRef]
24. Martinez-Cisneros, C.; Antonelli, C.; Levenfeld, B.; Varez, A.; Pérez-Flores, J.C.; Santos-Méndez, A.; Kuhn, A.; Sanchez, J.Y. Non-woven polyaramid porous membranes as separators for Li-ion batteries? *Electrochim. Acta* **2021**, *390*, 138835. [CrossRef]
25. Deng, C.; Jiang, Y.; Fan, Z.; Zhao, S.; Ouyang, D.; Tan, J.; Zhang, P.; Ding, Y. Sepiolite-based separator for advanced Li-ion batteries. *Appl. Surf. Sci.* **2019**, *484*, 446–452. [CrossRef]
26. Yang, Y.; Huang, C.; Gao, G.; Hu, C.; Luo, L.; Xu, J. Aramid nanofiber/bacterial cellulose composite separators for lithium-ion batteries. *Carbohydr. Polym.* **2020**, *247*, 116702. [CrossRef] [PubMed]
27. Liu, M.-C.; Chen, H.-J.; Wu, G.; Wang, X.-L.; Wang, Y.-Z. Multifunctional robust aerogel separator towards high-temperature, large-rate, long-cycle lithium-ion batteries. *Chin. Chem. Lett.* **2022**. [CrossRef]
28. Sheng, L.; Li, Z.; Hsueh, C.-H.; Liu, L.; Wang, J.; Tang, Y.; Wang, J.; Xu, H.; He, X. Suppression of lithium dendrite by aramid nanofibrous aerogel separator. *J. Power Sources* **2021**, *515*, 230608. [CrossRef]
29. Manly, A.J.; Tenhaeff, W.E. One-step fabrication of robust lithium ion battery separators by polymerization-induced phase separation. *J. Mater. Chem. A* **2022**, *10*, 10557–10568. [CrossRef]
30. Wang, E.; Wu, H.-P.; Chiu, C.-H.; Chou, P.-H. The Effect of Battery Separator Properties on Thermal Ramp, Overcharge and Short Circuiting of Rechargeable Li-Ion Batteries. *J. Electrochem. Soc.* **2019**, *166*, A125–A131. [CrossRef]
31. Xu, K.; Qin, Y.; Xu, T.; Xie, X.; Deng, J.; Qi, J.; Huang, C. Combining polymeric membranes with inorganic woven fabric: Towards the continuous and affordable fabrication of a multifunctional separator for lithium-ion battery. *J. Membr. Sci.* **2019**, *592*, 117364. [CrossRef]
32. Kalnaus, S.; Wang, Y.; Turner, J.A. Mechanical behavior and failure mechanisms of Li-ion battery separators. *J. Power Sources* **2017**, *348*, 255–263. [CrossRef]
33. Wang, Y.; Wang, Q.; Wei, X.; Song, Z.; Lan, Y.; Luo, W.; Yin, C.; Yue, Z.; Zhou, L.; Li, X. A novel three-dimensional boehmite nanowhiskers network-coated polyethylene separator for lithium-ion batteries. *Ceram. Int.* **2021**, *47*, 10153–10162. [CrossRef]
34. Li, Y.; Yu, L.; Hu, W.; Hu, X. Thermotolerant separators for safe lithium-ion batteries under extreme conditions. *J. Mater. Chem. A* **2020**, *8*, 20294–20317. [CrossRef]
35. Huang, X.; Hitt, J. Lithium ion battery separators: Development and performance characterization of a composite membrane. *J. Membr. Sci.* **2013**, *425–426*, 163–168. [CrossRef]
36. Qin, S.; Wang, M.; Wang, C.; Jin, Y.; Yuan, N.; Wu, Z.; Zhang, J. Binder-Free Nanoparticulate Coating of a Polyethylene Separator via a Reactive Atmospheric Pressure Plasma for Lithium-Ion Batteries with Improved Performances. *Adv. Mater. Interfaces* **2018**, *5*, 1800579. [CrossRef]
37. Dong, G.; Dong, N.; Liu, B.; Tian, G.; Qi, S.; Wu, D. Ultrathin inorganic-nanoshell encapsulation: TiO_2 coated polyimide nanofiber membrane enabled by layer-by-layer deposition for advanced and safe high-power LIB separator. *J. Membr. Sci.* **2020**, *601*, 117884. [CrossRef]
38. Wu, D.; Dong, N.; Wang, R.; Qi, S.; Liu, B.; Wu, D. In situ construction of High-safety and Non-flammable polyimide "Ceramic" Lithium-ion battery separator via SiO_2 Nano-Encapsulation. *Chem. Eng. J.* **2021**, *420*, 129992. [CrossRef]
39. Shi, C.; Zhang, P.; Huang, S.; He, X.; Yang, P.; Wu, D.; Sun, D.; Zhao, J. Functional separator consisted of polyimide nonwoven fabrics and polyethylene coating layer for lithium-ion batteries. *J. Power Sources* **2015**, *298*, 158–165. [CrossRef]
40. Kim, Y.; Lee, W.-Y.; Kim, K.J.; Yu, J.-S.; Kim, Y.-J. Shutdown-functionalized nonwoven separator with improved thermal and electrochemical properties for lithium-ion batteries. *J. Power Sources* **2016**, *305*, 225–232. [CrossRef]
41. Delaporte, N.; Perea, A.; Paolella, A.; Dubé, J.; Vigeant, M.-J.; Demers, H.; Clément, D.; Zhu, W.; Gariépy, V.; Zaghib, K. Alumina-flame retardant separators toward safe high voltage Li-Ion batteries. *J. Power Sources* **2021**, *506*, 230189. [CrossRef]

42. He, H.; Wang, X.; Liu, W. Effects of PEGDMA on a PET non-woven fabric embedded PAN lithium-ion power battery separator. *Solid State Ion.* **2016**, *294*, 31–36. [CrossRef]
43. Xu, Q.; Kong, Q.; Liu, Z.; Wang, X.; Liu, R.; Zhang, J.; Yue, L.; Duan, Y.; Cui, G. Cellulose/Polysulfonamide Composite Membrane as a High Performance Lithium-Ion Battery Separator. *ACS Sustain. Chem. Eng.* **2014**, *2*, 194–199. [CrossRef]
44. Tan, L.; Li, Z.; Shi, R.; Quan, F.; Wang, B.; Ma, X.; Ji, Q.; Tian, X.; Xia, Y. Preparation and Properties of an Alginate-Based Fiber Separator for Lithium-Ion Batteries. *ACS Appl. Mater. Interfaces* **2020**, *12*, 38175–38182. [CrossRef]
45. Miao, Y.-E.; Zhu, G.-N.; Hou, H.; Xia, Y.-Y.; Liu, T. Electrospun polyimide nanofiber-based nonwoven separators for lithium-ion batteries. *J. Power Sources* **2013**, *226*, 82–86. [CrossRef]
46. Liu, K.; Liu, W.; Qiu, Y.; Kong, B.; Sun, Y.; Chen, Z.; Zhuo, D.; Lin, D.; Cui, Y. Electrospun core-shell microfiber separator with thermal-triggered flame-retardant properties for lithium-ion batteries. *Sci. Adv.* **2017**, *3*, e1601978. [CrossRef]
47. Wang, L.; Wang, Z.; Sun, Y.; Liang, X.; Xiang, H. Sb_2O_3 modified PVDF-CTFE electrospun fibrous membrane as a safe lithium-ion battery separator. *J. Membr. Sci.* **2019**, *572*, 512–519. [CrossRef]
48. Feng, L.; Zhang, X.; Chen, Y.; Jiang, L. Study of making lithium ion battery separator by wet non-woven papermaking. *Membr. Sci. Tech.* **2017**. [CrossRef]
49. Sheng, J.; Chen, T.; Wang, R.; Zhang, Z.; Hua, F.; Yang, R. Ultra-light cellulose nanofibril membrane for lithium-ion batteries. *J. Membr. Sci.* **2020**, *595*, 117550. [CrossRef]
50. Xie, W.; Liu, W.; Dang, Y.; Tang, A.; Deng, T.; Qiu, W. Investigation on electrolyte-immersed properties of lithium-ion battery cellulose separator through multi-scale method. *J. Power Sources* **2019**, *417*, 150–158. [CrossRef]